Structural Eng./Earthquake Eng., JSCE, Vol.17, No.1, 1s-13s, 2000 January
(J. Struct. Mech. Earthquake Eng., JSCE, No. 640/ I -50)

ENERGY RELEASE RATES FOR INTERFACIAL CRACK IN LAMINATED STRUCTURES

Hong YUAN[1] and Zhishen WU[2]

[1]Ph. D., Dept. of Urban and Civil Engineering, Ibaraki University
(Nakanarusawa 4-12-1, Hitachi 316-8511, Japan)
[2]Member of JSCE, Dr. Eng., Associate Professor, Dept. of Urban and Civil Engineering, Ibaraki University
(Nakanarusawa 4-12-1, Hitachi 316-8511, Japan)

According to elastic beam theory, in this paper the energy release rate is derived and calculated without the need of a detailed analysis of the crack-tip stress and displacement fields and it is then successfully partitioned into two parts which can reflect the mode I and mode II components. The partitioning of this total value is especially significant because there is considerable ambiguity regarding the values of the energy release rate components at the tip of a crack lying along the interface between two dissimilar isotropic media. An application of the basic solution for concrete structures strengthened with steel or FRP plates is made to illustrate its utility.

Key Words *: energy release rate, steel plate, FRP, interfacial crack, elastic laminate*

1. INTRODUCTION

The use of steel and fibre reinforced polymer (FRP) materials in the form of plate bonded to the tension face of reinforced concrete is becoming an increasing attractive solution to the strengthening of existing structures. Central to the performance of the strengthened concrete structures is the transfer of stresses from concrete to the steel or FRP plates through a thin adhesive layer. An important failure mode for such composite laminates is the delaminations or debondings due to the unstable propagation of interfacial cracking initiating from various kinds of interlaminar defects. Such delaminations lead to a loss of stiffness and load-carrying capacity in a sudden manner. Therefore, the fracture mechanics based on energy consideration is considered to be very powerful for evaluating the load-carrying capacity of the composite structures. And a suitable method to calculate the energy release rate, G, is necessary.

There is a considerable literature of numerical analyses to calculate the energy release rate. Most use finite elements and then compute the energy release rate by various schemes based on node forces[1), 2)]. The results are rather complex to interpret and it seems there is scope for exploring analytical methods which can give a clearer insight into this problem. In the theoretical investigation of the delamination of laminated beams, simple beam theory has been found to be effective. A general method is given by Williams[3)] for calculating the energy release rate from the local value of bending moments and loads in a cracked laminate. This total value is then partitioned into mode I and II components. But the research is only restricted to laminated beam composed of the same material. Triantafillou and Gibson[4)] calculate the energy release rate for structural sandwich beams with isotropic faces and a foam core. Suo and Hutchinson[5)] give the expression of energy release rate for the split beam with a unit width subjected to general stretching and bending. But the shear deformation is not included in their discussion.

Toya[6] obtains mode I and II components of the energy release rate which are expressed in terms of the functions of the length of the incremental crack extension Δa. It is found that values of $G_I/\Delta a$ and $G_{II}/\Delta a$ oscillate violently when Δa approaches zero and that, hence, in contrast with the case for homogeneous materials, each energy release rate should be defined as $G_I/\Delta a$ and $G_{II}/\Delta a$ for an actual crack growth step size. Toya et al.[7] analyze asymmetric three-point bending of a layered beam with an interface crack by regarding the cracked part as two lapped beams hinged at both ends. The compliance and the total energy release rate are then derived.

The paper studies layered composite laminate with dissimilar materials by developing the general method given by Williams[3]. The energy release rate is calculated from the local values of bending moments, shear and axial loads. This total value is then partitioned into mode I and II components. Examples are given of the analysis of several geometry specimens including both variable and constant ratio mixed mode tests. There is some discussion of specimen compliance and stability criteria for fixed load and fixed displacement. Finally, some numerical results are given for simply supported beams strengthened with steel and FRP plates.

2. FORMULAS OF CALCULATION

In what follows we will consider a delamination as shown in **Fig. 1**. The model beam is formed by bonding two isotropic and linearly elastic rectangular beams having the same width b. Thicknesses of the two layers are h_1 and h_2 for the upper and lower strip, respectively. Poisson's ratios and Young's moduli of the two layers are ν_1 and E_1 for the upper strip and ν_2 and E_2 for the lower strip, respectively.

From elastic beam theory and plane section assumption, we can easily obtain stress distribution in the laminated beam

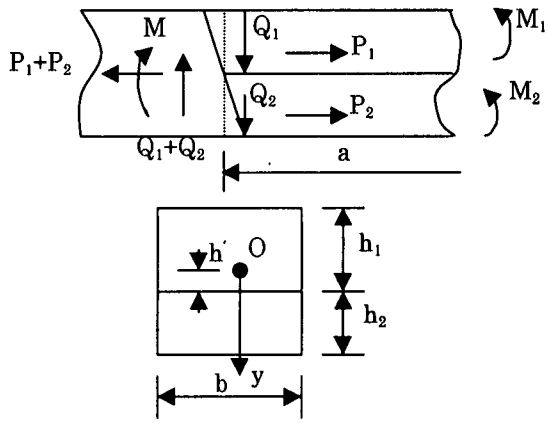

Fig. 1 Loads at crack tip

$$\sigma_1 = \frac{ME_1}{D'}y \quad , \quad \tau_1 = \frac{QE_1}{2D'}[(h_1 - h')^2 - y^2]$$

$$-(h_1 - h') \le y \le h'$$

$$\sigma_2 = \frac{ME_2}{D'}y \quad , \quad \tau_2 = \frac{QE_2}{2D'}[(h' + h_2)^2 - y^2]$$

$$h' < y \le h_2 + h' \qquad (1)$$

where $D' = E_1 I_1' + E_2 I_2'$ is the flexural rigidity of the composite beam. I_1' and I_2' are the second moment of inertia of the upper and lower beam with respect to the neutral axis of the composite beam, with h' being the distance of the neutral axis from interface

$$I_1' = \frac{1}{12}bh_1^3 + bh_1(\frac{h_1}{2} - h')^2$$

$$I_2' = \frac{1}{12}bh_2^3 + bh_2(\frac{h_2}{2} + h')^2$$

$$h' = \frac{E_1h_1^2 - E_2h_2^2}{2(E_1h_1 + E_2h_2)} \qquad (2)$$

$$Q = Q_1 + Q_2$$

$$M = M_1 + M_2 - P_1(\frac{h_1}{2} - h') + P_2(\frac{h_2}{2} + h') \qquad (3)$$

Assume that the crack growth is δa, then G may be defined as

$$G = \frac{1}{b}\left(\frac{dU_e}{da} - \frac{dU_s}{da}\right) \qquad (4)$$

where U_e is the external work performed and U_s is the strain energy. According to the bending moments M_1 and M_2, axial loads P_1 and P_2, and shear forces Q_1 and Q_2 applied to the upper and lower sections at the crack tip respectively, and using the similar derivation as in 3), we may write the expression for G as

$$G = \frac{1}{2b}\left\{\frac{M_1^2}{E_1 I_1} + \frac{M_2^2}{E_2 I_2} - \frac{\left[M_1 + M_2 - P_1\left(\frac{h_1}{2} - h'\right) + P_2\left(\frac{h_2}{2} + h'\right)\right]^2}{D'}\right\}$$

$$+ \frac{6}{5}\cdot\frac{1+\nu_1}{E_1}\cdot\frac{Q_1^2}{b^2 h_1} + \frac{6}{5}\cdot\frac{1+\nu_2}{E_2}\cdot\frac{Q_2^2}{b^2 h_2}$$

$$- \frac{(Q_1+Q_2)^2}{4D'^2}\cdot E_1(1+\nu_1)\left[(h_1-h')^4 h_1 - \frac{2}{3}(h_1-h')^2 h'^3 - \frac{7}{15}(h_1-h')^5 + \frac{1}{5}h'^5\right]$$

$$- \frac{(Q_1+Q_2)^2}{4D'^2}\cdot E_2(1+\nu_2)\left[(h_2+h')^4 h_2 + \frac{2}{3}(h_2+h')^2 h'^3 - \frac{7}{15}(h_2+h')^5 - \frac{1}{5}h'^5\right]$$

$$+ \frac{1}{2b}\cdot\frac{P_1^2}{E_1 A_1} + \frac{1}{2b}\cdot\frac{P_2^2}{E_2 A_2} - \frac{1}{2b}\cdot\frac{(P_1+P_2)^2}{E_1 A_1 + E_2 A_2} \quad (5)$$

3. MODE PARTITIONING

This analysis is concerned with the calculation of G and not with criteria of fracture, however, when these are examined there is considerable evidence that the critical values of G are different for the opening mode I and the sliding mode II [8]. It is therefore necessary to separate, or partition, the total G calculated in the previous section into the opening component G_I and the sliding, or shear, component G_{II}.

Considering the moment case first, we may note that pure mode II is obtained when the curvature in the two arms is the same so that if we take notation

$$\psi_M = \frac{E_2 I_2}{E_1 I_1}$$

and we have M_{II} on the upper arm and $\psi_M M_{II}$ on the lower , then pure mode II is obtained. The opening mode only requires moments in opposite senses so we have M_I on the upper arm and $-M_I$ on the lower beam so that the applied moments may be resolved as

$$\begin{aligned} M_1 &= M_{II} + M_I \\ M_2 &= \psi_M M_{II} - M_I \end{aligned} \quad (6)$$

Axial forces from the uniform strain situation give only mode I and mode II arise solely from the opposite axial forces. We may write

$$\begin{aligned} P_1 &= P_I + P_{II} \\ P_2 &= \psi_P P_I - P_{II} \\ \psi_P &= \frac{E_2 A_2}{E_1 A_1} \end{aligned} \quad (7)$$

Shear forces from the uniform strain situation give rise to mode II only and opposite shear forces give mode I , so

$$\begin{aligned} Q_1 &= Q_{II} - Q_I \\ Q_2 &= \psi_Q Q_{II} + Q_I \\ \psi_Q &= \frac{1+\nu_1}{1+\nu_2}\cdot\frac{E_2 h_2}{E_1 h_1} \end{aligned} \quad (8)$$

Substitute the expressions of M_1 and M_2, P_1 and P_2, Q_1 and Q_2 into (5). We have

$$G = G_I + G_{II} \quad (9)$$

where G_I and G_{II} are mode I and II components of energy release rate, respectively. G_I is related with mode I components M_I, Q_I, P_I only and G_{II} is associated with mode II components M_{II}, Q_{II}, P_{II}

$$G_I = \frac{1}{2bE_2 I_2}\cdot(1+\psi_M)M_I^2 + \frac{6(1+\nu_2)}{5b^2 E_2 h_2}\cdot(1+\psi_Q)Q_I^2$$

$$G_{II} = \frac{1}{2bE_1I_1}\cdot(1+\psi_M)M_{II}^2$$

$$-\frac{1}{2bD'}\cdot\left[(1+\psi_M)M_{II} - \frac{h_1+h_2}{2}P_{II}\right]^2$$

$$+\frac{1}{2b^2E_2h_2}(1+\psi_P)P_{II}^2 + \left\{\frac{6(1+\nu_1)}{5b^2E_1h_1}\cdot(1+\psi_Q)\right.$$
$$-\frac{(1+\psi_Q)^2(1+\nu_1)E_1}{4D'^2}\cdot\left[(h_1-h')^4h_1\right.$$
$$-\frac{2}{3}(h_1-h')^2h'^3 - \frac{7}{15}(h_1-h')^5 + \frac{1}{5}h'^5\left.\right]$$
$$-\frac{(1+\psi_Q)^2(1+\nu_2)E_2}{4D'^2}\cdot\left[(h_2+h')^4h_2\right.$$
$$\left.\left.+\frac{2}{3}(h_2+h')^2h'^3 - \frac{7}{15}(h_2+h')^5 - \frac{1}{5}h'^5\right]\right\}Q_{II}^2 \qquad (10)$$

where

$$M_I = \frac{\psi_M M_1 - M_2}{1+\psi_M}$$

$$M_{II} = \frac{M_1+M_2}{1+\psi_M}$$

$$Q_I = \frac{Q_2 - \psi_Q Q_1}{1+\psi_Q}$$

$$Q_{II} = \frac{Q_1+Q_2}{1+\psi_Q}$$

$$P_I = \frac{P_1+P_2}{1+\psi_P}$$

$$P_{II} = \frac{\psi_P P_1 - P_2}{1+\psi_P}$$

$$Q_1 = -\frac{dM_1}{da}$$

$$Q_2 = -\frac{dM_2}{da}$$

When the lower beam is very thin, for example, the FRP sheet, then $h_2 << h_1$, $1+\psi_M \approx 1$, $1+\psi_Q \approx 1$, $1+\psi_P \approx 1$, and (10) can be simplified to

$$G_I = \frac{1}{2bE_2I_2}\cdot(\psi_M M_1 - M_2)^2$$
$$+\frac{6(1+\nu_2)}{5b^2E_2h_2}\cdot(Q_2-\psi_Q Q_1)^2$$

$$G_{II} = \frac{1}{2bE_1I_1}\cdot(M_1+M_2)^2$$
$$-\frac{1}{2bD'}\cdot\left[(M_1+M_2) - \frac{h_1}{2}(\psi_P P_1 - P_2)\right]^2$$
$$+\frac{1}{2b^2E_2h_2}\cdot(\psi_P P_1 - P_2)^2 + \left\{\frac{6(1+\nu_1)}{5b^2E_1h_1}\right.$$
$$-\frac{(1+\nu_1)E_1}{4D'^2}\cdot\left[(h_1-h')^4h_1 - \frac{2}{3}(h_1-h')^2h'^3\right.$$
$$\left.-\frac{7}{15}(h_1-h')^5 + \frac{1}{5}h'^5\right]$$
$$-\frac{(1+\nu_2)E_2}{4D'^2}\cdot\left[(h_2+h')^4h_2 + \frac{2}{3}(h_2+h')^2h'^3\right.$$
$$\left.\left.-\frac{7}{15}(h_2+h')^5 - \frac{1}{5}h'^5\right]\right\}(Q_1+Q_2)^2 \qquad (11)$$

4. MODE TEST EXAMPLES

(1) DCB Tests

The most common test of a double cantilever beam is shown in **Fig. 2**. For a centrally cracked section and for symmetrical loading, as shown in **Fig. 2**(a), we have $M_1 = Pa$, $M_2 = -Pa$, $Q_2 = -Q_1 = P$, giving $M_I = Pa$, $M_{II} = 0$, $Q_I = P$, $Q_{II} = 0$, so

$$G_I = \frac{6P^2a^2}{E_1b^2h_1^3}\left[1+\frac{1+\nu_1}{5}\left(\frac{h_1}{a}\right)^2\right]$$
$$+\frac{6P^2a^2}{E_2b^2h_2^3}\left[1+\frac{1+\nu_2}{5}\left(\frac{h_2}{a}\right)^2\right]$$

$$G_{II} = 0 \qquad (12)$$

For the lower beam with very thin thickness, (12)

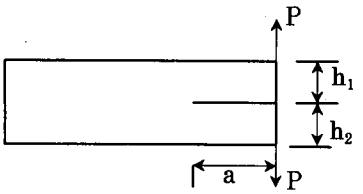

a) mode I

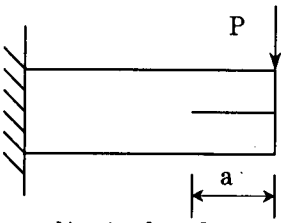

b) mixed mode

Fig. 2 Double cantilever beam (DCB) test

can reduce to

$$G_I = \frac{6P^2a^2}{E_2b^2h_2^3}\left[1+\frac{1+\nu_2}{5}\left(\frac{h_2}{a}\right)^2\right] \qquad (13)$$

For mixed mode shown in **Fig. 2**(b), assuming that the upper and lower beams contact each other only at free end, then we have the force between the two beams

$$P_1 = \frac{\psi_M}{1+\psi_M}P$$

and

$$M_1 = -Pa/(1+\psi_M)$$

$$M_2 = -\psi_M Pa/(1+\psi_M)$$

$$Q_1 = P/(1+\psi_M)$$

$$Q_2 = \psi_M P/(1+\psi_M)$$

and finally

$$M_I = 0$$

$$M_{II} = -Pa/(1+\psi_M)$$

$$Q_I = \left(\frac{1}{1+\psi_Q}-\frac{1}{1+\psi_M}\right)P$$

$$Q_{II} = \frac{1}{1+\psi_Q}P$$

The results for G are

$$G_I = \frac{6(1+\nu_2)}{5b^2E_2h_2}\cdot(1+\psi_Q)\frac{(\psi_M-\psi_Q)^2}{(1+\psi_Q)^2(1+\psi_M)^2}P^2$$

$$G_{II} = \frac{1}{2bE_2I_2}\cdot\frac{\psi_M}{1+\psi_M}P^2a^2$$

$$-\frac{P^2a^2}{2bD'}\left\{\frac{6(1+\nu_1)}{5b^2E_1h_1}\cdot\frac{1}{(1+\psi_Q)}\right.$$

$$-\frac{(1+\nu_1)E_1}{4D'^2}\cdot\left[(h_1-h')^4h_1-\frac{2}{3}(h_1-h')^2h'^3\right.$$

$$\left.-\frac{7}{15}(h_1-h')^5+\frac{1}{5}h'^5\right]$$

$$-\frac{(1+\nu_2)E_2}{4D'^2}\cdot\left[(h_2+h')^4h_2+\frac{2}{3}(h_2+h')^2h'^3\right.$$

$$\left.\left.-\frac{7}{15}(h_2+h')^5-\frac{1}{5}h'^5\right]\right\}P^2 \qquad (14)$$

and neglecting the shear correction, we have pure mode II. In this case the expressions of G are largely simplified

$$G_I = 0$$

$$G_{II} = \frac{1}{2bE_2I_2}\cdot\frac{\psi_M}{1+\psi_M}P^2a^2-\frac{P^2a^2}{2bD'} \qquad (15)$$

For the lower beam with very thin thickness, (15) reduces to

$$G_{II} = \frac{1}{2b}\cdot\left(\frac{1}{E_1I_1}-\frac{1}{D'}\right)P^2a^2 \qquad (16)$$

(2) A Variable Ratio Mixed Test

The test shown in **Fig. 3** gives continuously varying ratio mixed mode testing. For $0 < a \le l$ we have

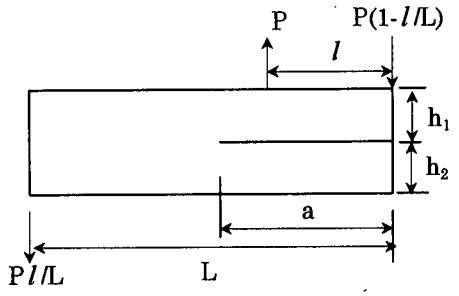

Fig. 3 Variable ratio mixed mode test

$$M_1 = -\frac{1}{1+\psi_M} Pa\left(1-\frac{l}{L}\right)$$

$$M_2 = -\frac{\psi_M}{1+\psi_M} Pa\left(1-\frac{l}{L}\right)$$

with

$$G_{II} = \frac{1}{2bE_2I_2}\cdot\frac{\psi_M}{1+\psi_M} P^2a^2\left(1-\frac{l}{L}\right)^2$$

$$-\frac{1}{2bD'} P^2a^2\left(1-\frac{l}{L}\right)^2$$

and $G_I = 0$, i.e., pure mode II.

For $l \le a \le L$, the force between the two beams is

$$P_1 = \frac{\psi_M}{1+\psi_M}\left(\frac{3}{2}\left(\frac{l}{a}\right)-\frac{1}{2}\left(\frac{l}{a}\right)^3-\frac{l}{L}\right)$$

and $M_1 = -Pl(1-a/L)+P_1 a$, $M_2 = -P_1 a$, finally

$$M_I = \frac{1}{2}\cdot\frac{\psi_M}{1+\psi_M} Pl\left(1-\frac{l^2}{a^2}\right)$$

$$M_{II} = -\frac{1}{1+\psi_M} Pl\left(1-\frac{a}{L}\right)$$

The results for G are

$$G_I = \frac{1}{8bE_2I_2}\cdot\frac{\psi_M^2}{1+\psi_M} P^2l^2\left(1-\frac{l^2}{a^2}\right)^2$$

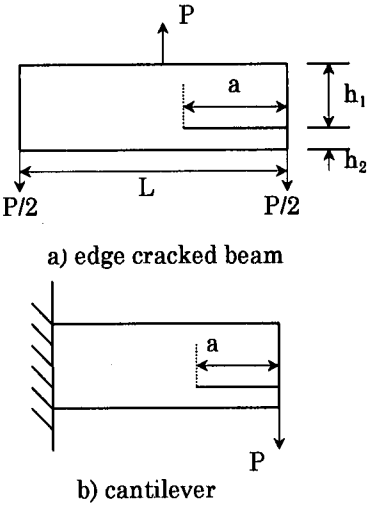

Fig. 4 Fixed ratio mixed mode tests

$$G_{II} = \frac{1}{2bE_2I_2}\cdot\frac{\psi_M}{1+\psi_M} P^2l^2\left(1-\frac{a}{L}\right)^2$$

$$-\frac{1}{2bD'} P^2l^2\left(1-\frac{a}{L}\right)^2 \qquad (17)$$

For FRP sheet strengthened beam, we obtain

$$G_I = \frac{\psi_M}{8bE_1I_1}\cdot P^2l^2\left(1-\frac{l^2}{a^2}\right)^2$$

$$G_{II} = \frac{1}{2b}\cdot\left(\frac{1}{E_1I_1}-\frac{1}{D'}\right)P^2l^2\left(1-\frac{a}{L}\right)^2 \qquad (18)$$

At $a = l$ we have pure mode II and at $a = L$ pure mode I so a complete variation in ratio is obtained on one specimen. We can also notice that G_I increases as a increases and G_{II} decreases as a increases.

(3) Fixed Ratio Mixed Mode Test

Fig. 4(a) shows a three point loaded edge cracked beam test with an off-centre crack and a loading system such that the moment on the upper arm is zero. Thus

$$M_1 = 0 \text{ and } M_2 = -\frac{1}{2}Pa$$

giving

$$M_I = -M_{II} = \frac{Pa}{2(1+\psi_M)}$$

$$G_I = \frac{1}{8bE_2I_2} \cdot \frac{1}{1+\psi_M} P^2a^2$$

$$G_{II} = \frac{1}{8bE_2I_2} \cdot \frac{\psi_M}{1+\psi_M} P^2a^2 - \frac{1}{8bD'} P^2a^2 \quad (19)$$

Thus the mixed mode ratio is

$$\frac{G_{II}}{G_I} = \frac{\frac{\psi_M}{1+\psi_M} - \frac{E_2I_2}{D'}}{\frac{1}{1+\psi_M}} \quad (20)$$

i.e., pure mode I at $h_2 \to 0$ and independent of a. For FRP sheet strengthened beam, we obtain

$$G_I = \frac{1}{8bE_2I_2} \cdot P^2a^2$$

$$G_{II} = \frac{1}{8b} \cdot \left(\frac{1}{E_2I_2} - \frac{1}{D'} \right) P^2a^2 \quad (21)$$

Fig. 4(b) shows a cantilever version of this test which is only a slight variation on the mode II test in **Fig. 2**(b). Here $M_1 = 0$ but $M_2 = -Pa$ and the results are four times those given in **Fig. 4**(a).

(4) Transverse Splitting From Notches

The general method developed here may be applied to the situation illustrated in **Fig. 5** in which the crack c runs normal to the notch. Such a configuration occurs when the notches are normal to the fibre direction in composites but the failure is transverse splitting normal to the notch and is a possible way of modeling damage.

For the case of tension a moment is induced on h_2 so that, $P_1 = 0$, $P_2 = P$, $M_1 = 0$ and $M_2 = -(h' + h_2/2)P$, this gives

$$P_I = -P_{II} = \frac{1}{1+\psi_P} P$$

$$M_I = -M_{II} = \frac{h' + \frac{h_2}{2}}{1+\psi_M} P$$

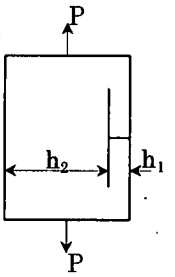

a) tension

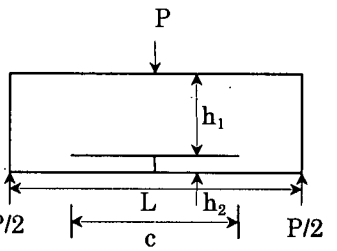

b) three point bending

Fig. 5 Transverse splitting from notches

$$G_I = \frac{1}{2bE_2I_2} \cdot \frac{\left(h' + \frac{h_2}{2} \right)^2}{1+\psi_M} P^2$$

$$G_{II} = \frac{1}{2bE_2I_2} \cdot \frac{\psi_M \left(h' + \frac{h_2}{2} \right)^2}{1+\psi_M} P^2$$

$$+ \frac{1}{2b^2E_2h_2} \cdot \frac{1}{1+\psi_P} P^2 \quad (22)$$

For the three point bend configuration shown in **Fig. 5**(b) the moments are $M_1 = P(L-c)/4$ and $M_2 = 0$, so that

$$G_I = \frac{1}{32bE_2I_2} \cdot \frac{\psi_M^2}{1+\psi_M} P^2(L-c)^2$$

$$G_{II} = \frac{1}{32bE_2I_2} \cdot \frac{\psi_M}{1+\psi_M} P^2(L-c)^2$$

$$- \frac{1}{32bD'} P^2(L-c)^2 \quad (23)$$

5. COMPLIANCE AND STABILITY

Most delamination tests measure load, crack length and load point displacement so the latter provides a method of determining EI independently or checking on the value of a if an expression for the compliance is known. This may be done using conventional beam theory directly but a more convenient method is via dC/da and the expression for G in terms of load

$$G = \frac{P^2}{2b} \cdot \frac{dC}{da}$$

i.e.

$$C = \int_0^a \frac{2bG}{P^2} da + C_0 \qquad (24)$$

where C_0 is the compliance with no crack present. For the mode I DCB in **Fig. 2**(a) we have

$$G = G_I = \frac{a^2}{2b}\left(\frac{1}{E_1 I_1} + \frac{1}{E_2 I_2}\right) P^2$$

since $C_0 = 0$ in this case. Here the shear correction is neglected. For a uniform specimen in which I_1 and I_2 are constants we have

$$C = \frac{1}{3} a^3 \left(\frac{1}{E_1 I_1} + \frac{1}{E_2 I_2}\right) = \frac{\delta}{P} \qquad (25)$$

and G_I may be written as

$$G_I = \frac{3}{2} \cdot \frac{P\delta}{ba} = \frac{1}{2b} \cdot \left[3P^2\delta\left(\frac{1}{E_1 I_1} + \frac{1}{E_2 I_2}\right)^{1/2}\right]^{2/3} \qquad (26)$$

Thus if EI is not known G_I may be obtained from P, δ and a and, if it is, then a check on the value of a used may be via P and δ.

Stability is an important factor in both testing and design and is controlled by the rate of change of G, i.e., dG/da. Practical behavior will be determined by material properties such as how G_c varies with a in resistance curve effects, but some special specimen conditions are important in all cases. It is often very convenient to have a test in which G does not vary with a ($dG/da = 0$) so that for a constant G_c value a driven crack will run at constant load. For the DCB mode I case, this is achieved when $\frac{a^2}{2b} \cdot \left(\frac{1}{E_1 I_1} + \frac{1}{E_2 I_2}\right) = \text{constant}$.

Specimens driven by stiff machines operate as constant displacement systems if the crack moves forward quickly. If dG/da is positive then this will tend to be unstable since G increases with a. (It may not necessarily be in practice, of course, since dG_c/da may also be positive). The condition of whether dG/da is positive or negative at constant δ, is, however, of practical interest and may be defined in general via

$$G = \frac{P^2}{2b} \cdot \frac{dC}{da} = \frac{\delta^2}{2bC^2} \cdot \frac{dC}{da} \qquad (27)$$

and the condition for stable growth

$$\left.\frac{dG}{da}\right|_{\delta = const} \le 0$$

is equivalent to

$$\Gamma = \frac{1}{2} \cdot \frac{C}{C'}\left(\frac{C''}{C'} - \frac{b'}{b}\right) \le 1 \qquad (28)$$

where $' = d/da$ etc. for case of $b = const$ it can be simplified

$$\Gamma = \frac{1}{2} \cdot \frac{CC''}{C'C'} \le 1 \qquad (29)$$

For the DCB mode I case with a uniform section

$$C = \frac{1}{3} a^3 \left(\frac{1}{E_1 I_1} + \frac{1}{E_2 I_2}\right)$$

i.e., $\Gamma = 1/3$, and the fracture is stable. It is easy to verify that fracture is again stable when shear correction is considered.

For the mode II DCB test, **Fig. 2**(b)

$$G = \frac{1}{2b}\left(\frac{1}{E_2 I_2} \cdot \frac{\psi_M}{1+\psi_M} - \frac{1}{D'}\right) P^2 a^2$$

$$C = \frac{1}{3} a^3 \left(\frac{1}{E_2 I_2} \cdot \frac{\psi_M}{1+\psi_M} - \frac{1}{D'}\right) + \frac{L^3}{3D'}$$

$$\Gamma = \frac{\frac{D'}{E_2 I_2}\cdot\frac{\psi_M}{1+\psi_M} - 1 + \frac{L^3}{a^3}}{3\left(\frac{D'}{E_2 I_2}\cdot\frac{\psi_M}{1+\psi_M} - 1\right)}, \quad 0 < \frac{a}{L} < 1 \qquad (30)$$

i.e. stable for

$$\left[2\left(\frac{D'}{E_2 I_2}\cdot\frac{\psi_M}{1+\psi_M} - 1\right)\right]^{-1/3} \le \frac{a}{L} < 1, \ \Gamma \le 1,$$

and unstable for

$$0 < \frac{a}{L} < \left[2\left(\frac{D'}{E_2 I_2}\cdot\frac{\psi_M}{1+\psi_M} - 1\right)\right]^{-1/3}, \ \Gamma > 1,$$

For the case of $E_1 = E_2$ and $h_1 = h_2$ the result is

$$0.550 \le \frac{a}{L} < 1, \qquad \text{stable}$$

$$0 < \frac{a}{L} < 0.550, \qquad \text{unstable}$$

For the fixed ratio mixed mode test shown in **Fig. 4**(b) we have

$$G = G_I + G_{II} = \frac{1}{2b}\left(\frac{1}{E_2 I_2} - \frac{1}{D'}\right)P^2 a^2$$

$$C = \frac{1}{3}a^3\left(\frac{1}{E_2 I_2} - \frac{1}{D'}\right) + \frac{L^3}{3D'} \qquad (31)$$

Here we have

$$\Gamma = \frac{\frac{D'}{E_2 I_2} - 1 + \frac{L^3}{a^3}}{3\left(\frac{D'}{E_2 I_2} - 1\right)}, \quad 0 < \frac{a}{L} < 1 \qquad (32)$$

Let

$$\alpha = \left[2\left(\frac{D'}{E_2 I_2} - 1\right)\right]^{-1/3}$$

For $\alpha \ge 1$ the growth is all unstable but for $\alpha < 1$ there is a transition from unstable to stable behavior as the crack grows.

Finally, for the transverse splitting cases discussed in Section 4.4 we may note that in the tension case G is not a function of the crack length so that C is a linear function of crack length, $\Gamma = 0$ and the test is always stable. For the constant load systems we have $dG/da = 0$ and the test is also always stable. In bending G decreases as crack length grows and thus the test is stable for both constant load and constant displacement cases.

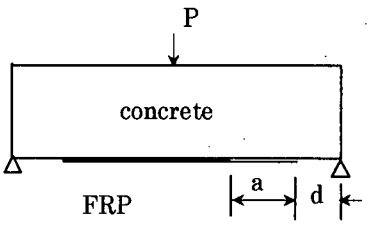

Fig.6 Debonding at the tip of a bonded reinforcement

6. ENERGY RELEASE RATES IN BEAMS STRENGTHENED WITH FRP OR STEEL PLATE

The practical utility of the proposed method is illustrated by several examples of concrete beams strengthened by FRP and steel plates. Although FRP sheet is not isotropic, we conclude that the method in this paper can be used to study FRP-strengthened beam since the bending moment and shear force in FRP are very small and can be neglected. Materials chosen are concrete with Young's modulus of $E_1 = 3.25\times10^5\,\text{kg/cm}^2$, and Poisson's ratio of $\nu_1 = 0.16$ for the upper beam and FRP plate with $E_2 = 2.3\times10^6\,\text{kg/cm}^2$ and $\nu_2 = 0.3$ or high modulus type of FRP plate with $E_2' = 5.45\times10^6\,\text{kg/cm}^2$ and $\nu_2' = 0.3$ for the lower beam. The thickness $h_1 = 15\,\text{cm}$, width $b = 10\,\text{cm}$, and span $l = 75\,\text{cm}$ are chosen. The unit load $P = 1\,\text{kg}$ is applied at the center of the beam.

(1) Debonding at the Tip of a Bonded Reinforcement

Using above method we obtain

$$M_1 = \frac{1}{2}P(a+d), \ M_2 = 0$$

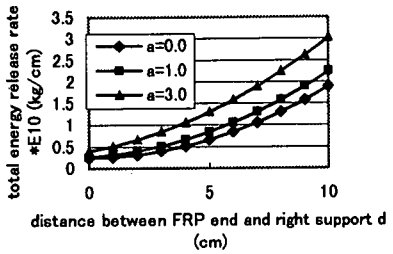

Fig. 7 Variation of energy release rate with distance d

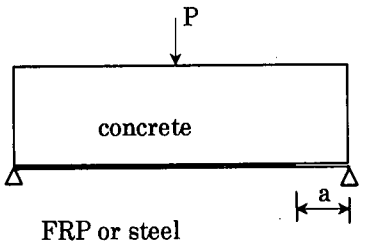

Fig. 8 A laminated beam containing an edge crack

$$Q_1 = -\frac{P}{2},\ Q_2 = 0$$

so that we obtain the total energy release rate of FRP strengthened plate as shown in **Fig. 7**. Here the thickness of FRP plate is 0.1 cm. From **Fig. 7** we conclude that for a certain fixed value of a, energy release rate increases as d increases, and so when used to strengthening concrete beam, FRP should be bonded on the whole tension face as possible. Debonding is more likely to occur for a shorter FRP length. The same conclusion can be obtained for beam strengthened with steel plates.

(2) Laminated Beam Containing an Edge Crack

As is shown in **Fig. 8**, an edge local delamination occurs. We have

$$M_1 = \frac{Pa}{2(1+\psi_M)}$$

$$M_2 = \frac{\psi_M Pa}{2(1+\psi_M)}$$

$$Q_1 = -\frac{P}{2(1+\psi_M)}$$

$$Q_2 = -\frac{\psi_M P}{2(1+\psi_M)}$$

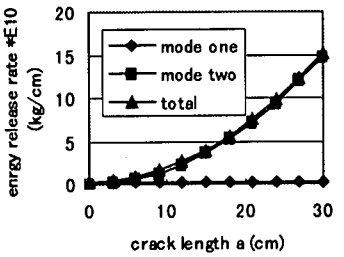

a) thickness of FRP=0.1cm

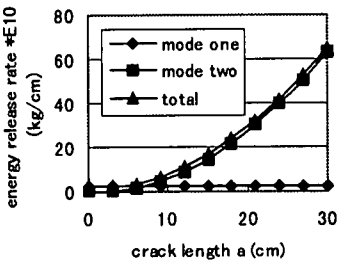

b) thickness of FRP=1cm

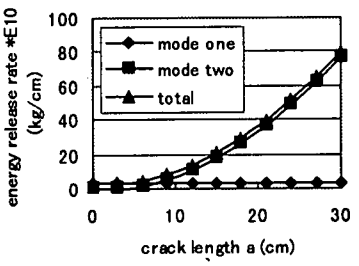

c) thickness of FRP=2cm

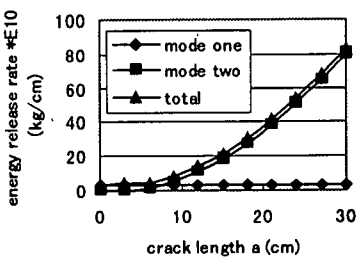

d) thickness of FRP=3cm

From these expressions and (10) we can easily obtain the energy release rate components and the total value as shown in **Fig. 9**.

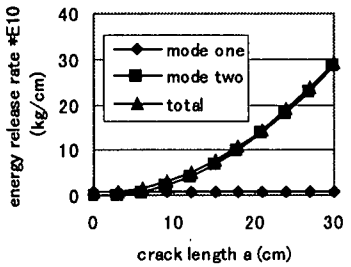

A) thickness of high strength FRP=0.1cm

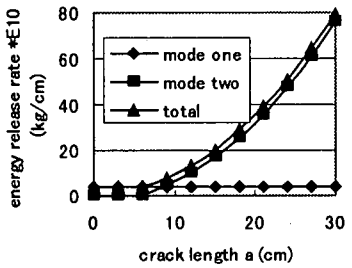

B) thickness of high strength FRP=1cm

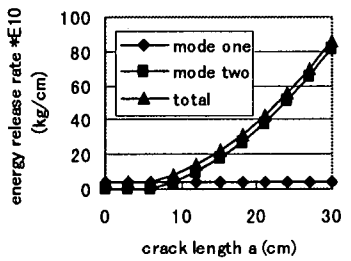

C) thickness of high strength FRP=2cm

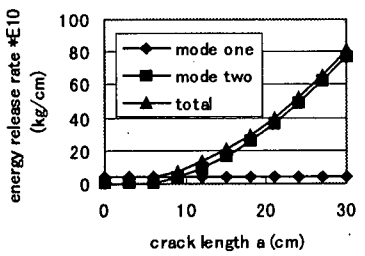

D) thickness of high strength FRP=3cm

Fig.9 Variation of energy release rate with crack length

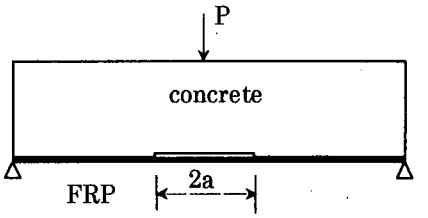

Fig. 10 A laminated beam containing an interface crack

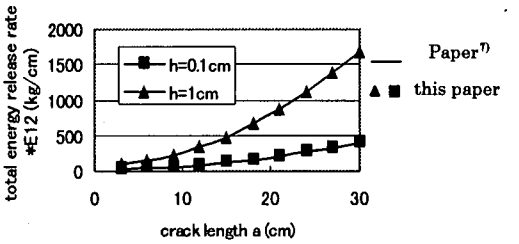

Fig.11 Comparison with reference[7]

It can be concluded from **Fig. 9** that energy release rates are almost the same for beams strengthened with FRP and steel plates because of similar Young's moduli and Poisson's ratios. Energy release rates increase as the increase of FRP thickness and crack length. It means that for thicker FRP and steel plates or longer interfacial crack debonding is easier to appear.

(3) Interface Crack Embedded in a Laminated Beam

Using the expression of internal forces obtained in reference[7], we can compare the numerical result of total energy release rate for FRP strengthened beam here with[7] as shown in **Fig. 11**. It is obvious that the curves are in good agreement. This confirms the accuracy of the analyses in this paper. Variations of energy release rate components and total value with crack length for FRP strengthened beam are shown in **Fig. 12**. It can also be seen that energy release rates increase as the increase of FRP thickness and crack length. However, further confirmation by making comparison investigations between the analysis and experimental findings is considered to be necessary, especially for the case of the structures strengthened with thin FRP sheets or plates, because the stress field is considerably localized.

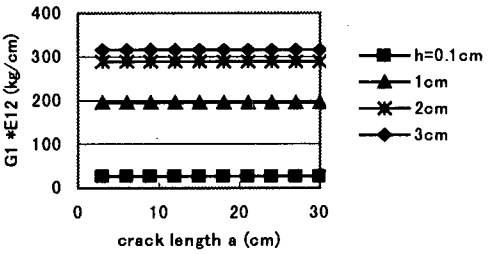

a) energy release rate of mode one

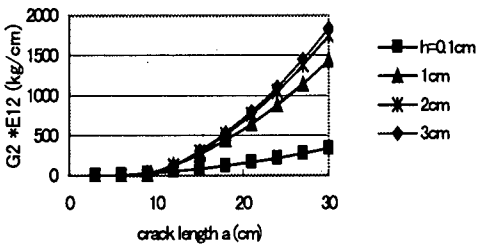

b) energy release rate of mode two

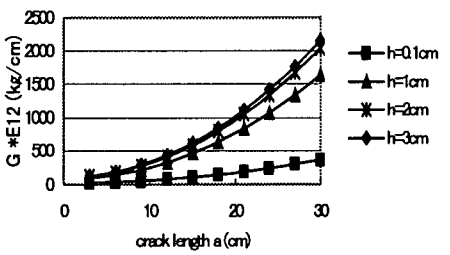

c) total energy release rate

Fig.12 Variation of energy release rate with crack length

7. CONCLUSIONS

The examples given cover most of the test geometry used in testing laminates and also suggest some useful configurations for mixed mode tests. In all cases the general method enables the G_I and G_{II} components to be found easily thus facilitating test method development and the exploration of mixed mode fracture criteria. Some insight into post crack propagation behavior can be deduced by considering the system compliance and associated stability criteria. Finally three-point bending of a simply supported layered beam with an internal interface crack or edge interfacial crack was analyzed. Concrete beam strengthened by FRP and steel plates belongs to this category. Numerical results show that the method in this paper possesses high accuracy.

REFERENCES

1) Hamoush, S. A. and Ahmad, S. H.: Debonding of steel plate-strengthened concrete beams, J. of Structural Engineering, ASCE, Vol. 116, pp. 356-370, 1990.
2) Wu, Z. S., Matsuzaki, T. and Tanabe, K.: Interface crack propagation in FRP strengthened concrete structures, In Non-Metallic (FRP) Reinforcement for Concrete Structures, Proc. 3rd Intern. Symp., Japan Concrete Institute, 1, pp. 319-326, 1997.
3) Williams, J. G: On the calculation of energy release rates for cracked laminates, International Journal of Fracture, Vol. 36, pp. 101-119, 1988.
4) Triantafillou, T. C. and Gibson, L. J.: Debonding in foam-core sandwich panels, Materials and Structures, Vol. 22, pp. 64-69, 1989.
5) Suo, Z. and Hutchinson, J. W.: Interface crack between two elastic layers, I. J. of Fracture, Vol. 43, pp. 1-18, 1990.
6) Toya, M.: On mode I and mode II energy release rates of an interface crack, I. J. of Fracture, Vol. 56, pp. 345-352, 1992.
7) Toya, M., Aritomi, M. and Chosa, A.: Energy release rates for an interface crack embedded in a laminated beam subjected to three-point bending, J. of Applied Mechanics, Vol. 64, pp. 375-382, 1997.
8) Johnson, W. S. and Mangalgiri, P. D.: Influnce of the resin on interlaminar mixed-mode fracture, Toughened Composites, ASTM STP 937, Norman, J. Johnston ed., American Society for Testing and Materials, Philadelphia, pp. 295-315, 1987.

(Received June 3, 1999)

積層複合構造物における界面き裂先端のエネルギ解放率

袁　鴻・呉　智深

き裂先端における詳細な応力・変位場を解析せず，一般的な弾性力学的梁の曲げ理論によって，積層接着界面き裂先端のエネルギ解放率を計算する陽的算定式を導いた．また，エネルギ解放率を mode Ⅰ および mode Ⅱ の二つの成分に分解し，積層接着界面の剥離特性に関する検討を行った．さらに，理論解析手法は異なる構造材の積層複合構造に適用されていることから，鋼板や連続繊維シートによって補強されたコンクリート構造物の界面き裂のエネルギ解放率の算定に応用され，その有効性が検討された．